Materials Science & Engineering A 712 (2018) 757–764

Contents lists available at ScienceDirect

Materials Science & Engineering A

journal homepage: www.elsevier.com/locate/msea

Precipitation kinetics and hardening mechanism in Al-Si solid solutions processed by high pressure solution treatment

Maowen Liu[a], Hui Fu[b], Cong Xu[a], Wenlong Xiao[a,*], Qiuming Peng[b], Hiroshi Yamagata[c], Chaoli Ma[a,*]

[a] Key Laboratory of Aerospace Advanced Materials and Performance of Ministry of Education, School of Materials Science and Engineering, Beihang University, Beijing 100191, China

[b] State Key Laboratory of Metastable Materials Science and Technology, Yanshan University, Qinhuangdao 066004, China

[c] Center for Advanced Die Engineering and Technology, Gifu University, 1-1 Yanagido, Gifu City, Gifu 501-1193, Japan

ARTICLE INFO

Keywords:
Al-Si alloys
Si nanoparticles
Precipitation kinetics
Precipitation strengthening
High supersaturation

ABSTRACT

A dense uniform distribution of nanoscale Si precipitates in Al-Si binary alloys were achieved using high pressure solution treatment and aging treatment. Precipitation kinetics, hardening effect as well as supersaturation-growth-hardening relationships during aging treatment were quantitatively investigated. The results reveal that there exists a critical supersaturation value (0.026) during precipitation process, which divides the size versus time curve into two stages corresponding to different slopes. The sudden variation in the curve around the critical point indicates a great change in the growth rate of second phase, which is assumed to be related to the inconstancy of diffusion coefficient over a wide supersaturation range. The dense nanoscale precipitates could lead to extraordinarily high precipitation strengthening, which is combined with solid solution hardening caused by residual Si solute atoms in Al matrix, resulting in much more complicated age hardening response than that in low solubility alloys. Ultra-high hardness (~ 130 HV) is achieved in Al-7Si alloy with optimized microstructure. This work provides a promising approach for achieving high performance alloys with nanoscale secondary phase as well as insights into the underlying mechanism of microstructure evolution during aging process.

1. Introduction

Al-Si cast alloys are widely used in automobile industry owing to their high strength to weight ratio, low coefficient of expansion, outstanding castability and excellent corrosion resistance [1,2]. The mechanical performance of Al-Si alloys is mainly decided by the morphology of Si phase, which significantly affects the initiation and propagation of cracks and fracture behavior of Al-Si alloys during deformation process [3,4]. Therefore, the modification and refinement of Si phase are crucial for improving mechanical properties and have attracted decades of lasting research efforts. As the most widely used method, the refinement effect of chemical modification is limited, restricting Si phase at micrometer level [5] which could hardly satisfy the ever-growing demand for high performance Al alloys. Recently, some attempts have been made to mechanically break Si phase into submicron particles using equal-channel angular pressing (ECAP) [6–8] and high-pressure torsion (HPT) [9–11], achieving certain magnitude of enhancement in mechanical properties of Al-Si alloys. Nevertheless, such methods were intended for pure metals or solid solutions rather than multi-phase alloys. The refinement of Si phase is less effective in comparison with that of Al matrix [6,8,9].

Compared to age-hardened alloys, Si solubility in Al matrix is very small and barely improves with increasing temperature [12], making it impossible to achieve dense nanoscale Si precipitates through high temperature solution treatment and aging treatment. On the other hand, pressure is another essential thermodynamic parameter whose effects on microstructure and phase composition [13] have long been neglected. With recent progress in high-pressure technique, considerable attention has been attracted by the probability to improve material performance using pressure treatment. Previous studies show that the solubility limit of Si in Al is extended beyond 15 at% at 5.4 GPa and can even reach 18 at% at 10 GPa [14,15] in comparison with only 1.5 at% at normal pressure [12], which makes it possible to form high density Si nanoparticles in Al-Si alloys during aging treatment.

In our preliminary research, the precipitation behaviors in Al-Si alloys with high Si solubility were found to be very different from their low Si solubility counterparts. In alloys with high Si solubility, the driving force for precipitation is much larger than that in alloys with

* Corresponding authors.
E-mail addresses: wlxiao@buaa.edu.cn (W. Xiao), machaoli@buaa.edu.cn (C. Ma).

https://doi.org/10.1016/j.msea.2017.12.033
Received 20 November 2017; Received in revised form 7 December 2017; Accepted 8 December 2017
Available online 09 December 2017
0921-5093/

low Si solubility [16,17], which would make a great difference on precipitation kinetics, significantly affecting precipitate morphologies as well as aging hardening response. Besides, the ultra-high residual Si solubility would give rise to extraordinarily high solid solution hardening [14], which would be combined with the precipitation hardening, making the hardening response much more complicated in high Si solubility alloys. Therefore, a clear and in-depth understanding of Si precipitation behavior and supersaturation-Si growth rate-hardening relationships are needed to control the morphology of Si precipitates as well as hardening effect in Al-Si solid solutions.

In the present work, Al-Si alloys with a dense uniform dispersion of nanoscale Si precipitates and extremely high hardness were prepared with high pressure solution treatment (HPST) followed by low temperature aging treatment. The evolution of microstructure and hardness during isothermal aging treatment were systematically investigated, based on which the supersaturation-growth-hardening relationships were quantitatively established. This work provides a promising approach for achieving high performance alloys with nanoscale secondary phase as well as insights into the underlying mechanism of microstructure evolution during aging process.

2. Experiments

Al-Si alloys with different Si contents (1.0 wt%, 3.0 wt%, 5.0 wt%, 7.0 wt%, hereafter in weight percentage) were prepared by conventional casting from 99.99 wt% pure Al and 99.999 wt% pure Si. The specimens were machined into cylinders with 10 mm in diameter and 12 mm in length for HPST, which was carried out in a cubic-anvil large-volume press with six rams [18]. The specimens were heated to 700 °C (eutectic temperature increases under high pressure [13]) under isostatic pressing (6 GPa) and held for 1 h followed by water quenching to room temperature. The HPST-processed specimens were taken into isothermal aging at 170 °C (the most widely used aging temperature for commercial Al-Si base alloy) for various periods using an oil bath. The preparation process is illustrated in Fig. 1.

Morphologies of the solution treated specimens were observed with an optical microscopy, and the microstructure evolution was characterized by an X-ray diffractometer (XRD) using Cu-Kα radiation with the wavelength of 0.15418 nm. Lattice parameters of Al matrix for specimens with different aging time were calculated from the XRD patterns according to the Nelson-Riley extrapolation procedure [19]. Details about the microstructure of Si precipitates were investigated by a transmission electron microscope (TEM) and scanning transmission electron microscope (STEM) operating at 200 kV. TEM specimens were prepared by electro-polishing in a solution of 30 vol% nitric acid and 70 vol% methanol, operating at 25 V and −30 °C. Vickers microhardness (HV) measurement was applied on the cross sections of specimens along 4 different radial directions by a hardness tester with a load of 0.49 N for a dwell time of 10 s.

3. Results

3.1. Solubility evolution

Fig. 2a shows the typical microstructure of as-cast Al-7Si alloy with coarse plate-like eutectic Si crystals distribute between the primary Al dendrites. After solution treatment under high pressure, the Si crystals

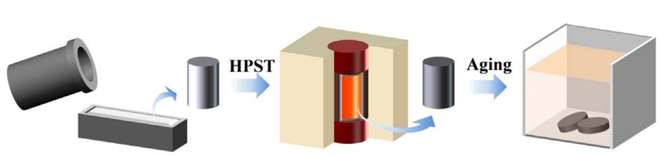

Fig. 1. Schematic illustration of sample fabrication, including casting, HPST and aging treatment.

fully dissolve in Al matrix and become invisible, as shown in Fig. 2b.

The XRD patterns in Fig. 3a display the microstructure evolution of Al-7Si alloy during HPST and isothermal aging treatment. The reflections of Si phase in the HPST-processed specimen disappear compared with that in the as-cast alloy, and then reappear in alloys with aging treatment. The broadened Si peaks in the aged alloys indicate the refinement of Si crystals. The peaks of Al phase slightly shift toward lower angles during aging treatment, indicating that the lattice parameters of Al matrix increase with increasing aging time which results from the decreasing solubility of Si in Al matrix. The atomic fractions of Si dissolved in Al matrix can be obtained from the linear relationship between Si solubility and Al lattice parameter [20], and the evolution of Si solubility with aging time is plotted in Fig. 3b. The curve reveals two stages up to 36000 s. It is evident that the Si solubility decreases rapidly until the time reaches 1800 s, and then the precipitation becomes slow. As no intermediate phases have been detected during precipitation of Si phase [21,22], it is regarded that all the reduced Si solute atoms transform to be Si crystals.

The fraction transformed as a function of time ($f(t)$) for the isothermal phase transformation involving nucleation and growth is generally described by the Johnson-Mehl-Avrami (JMA) equation [23]:

$$f(t) = 1 - \exp(-kt^n) \quad (1)$$

where k is the rate constant associates with growth rate and n is called Avrami exponent which is determined by the nucleation and growth mode. In general, Avrami exponent n can be achieved from the slope in the so-called Avrami plot ln[-ln(1-f)] versus ln$t$.

The Avrami plot of Si precipitation is inserted in Fig. 3b, where measured values deviate from the straight line. The deviation of the values during precipitation is generally regarded to be associated with k (growth rate), which reduces with the decreasing solubility [23]. Therefore, the slope at the initial stage of precipitation (low fraction transformed) is often used for analysis. In the present work, Avrami exponent n is calculated to be 1.3.

3.2. Morphology development

The STEM micrographs at low magnification in Fig. 4 show the morphologies of precipitates in alloys with different aging time. All the images are taken along [011] orientation of Al matrix. The inserted selected area electron diffraction (SAED) patterns contain Al (marked with arrows), Si and double diffraction spots, indicating that all the precipitates are Si crystals. The orientation of Si precipitates is identical to Al matrix, which is consistent with previous investigations [24,25]. A large amount of fine precipitates homogenously distribute in the matrix of the specimen aged for 300 s, as shown in Fig. 4a. By further aging, the precipitates grow rapidly within 1800 s, as shown in Fig. 4b-d. However, the growth of precipitates slowed down when the aging time is longer than 1800 s, as presented in Fig. 4e and f. The trend of growth rate revealed by Fig. 4 is consistent with the evolution of Si solubility in Fig. 3b.

Both equiaxed and plate-like Si precipitates are observed in Fig. 4. Precipitates are almost equiaxed in the specimen aged for 300 s, while some particles elongate parallel to $\{111\}_{Al}$ planes during aging process, as indicated by arrows in Fig. 4b and c. More elongated plates appear in the specimen aged for 1800 s, as shown in Fig. 4d. With longer aging time, the diameter of plates become larger while the thickness is almost unchanged (Fig. 4e-f), which results in high aspect ratio for the plate-like precipitates. The presence of equiaxed and plate-like Si precipitates during low temperature aging treatment was also reported in previous literatures [26,27], while the formation mechanism has been rarely investigated.

Details of the precipitates are presented in Fig. 5. Fig. 5a shows the microstructure of precipitates in the alloy aged for 600 s, where Moir é patterns (periodical network) arising from the overlapping of precipitates and matrix [24] can be observed. It seems that there are some